Lindemann parameters for solid membranes focused on carbon nanotubes

Jürgen Dietel
Institut für Theoretische Physik, Freie Universität Berlin, Arnimallee 14, D-14195 Berlin, Germany

Hagen Kleinert
Institut für Theoretische Physik, Freie Universität Berlin, Arnimallee 14, D-14195 Berlin, Germany and ICRANeT, Piazzale della Repubblica 1, 10-65122 Pescara, Italy

(Received 20 June 2008; revised manuscript received 18 August 2008; published 6 February 2009)

Temperature fluctuations in the normal direction of planar crystals such as graphene are quite violent and may be expected to strongly influence their melting properties. In particular, they will modify the Lindemann melting criterion. We calculate this modification in a self-consistent Born approximation. The result is applied to graphene and its wrapped version represented by single-walled carbon nanotubes. It is found that the out-of-plane fluctuations dominate over the in-plane fluctuations. This makes strong restrictions to possible Lindemann parameters. Astonishingly we find that these large out-of-plane fluctuations have only a small influence on the melting temperature.

DOI: 10.1103/PhysRevB.79.075412 PACS number(s): 61.46.Fg, 64.70.D−, 68.60.Dv, 87.16.D−

I. INTRODUCTION

The production of macroscopic two-dimensional (2D) graphene sheets by mechanical cleavaging[1] has demonstrated that free-standing or suspended 2D crystals can exist despite large positional fluctuations in two dimensions. Since then, a variety of other free-standing 2D crystallites has been prepared.[2] Wrapped versions of the 2D free-standing graphene had been found much earlier in 1991.[3] Recent observations[4] have confirmed the theoretical expectation that freely suspended graphene sheets are strongly undulated and behave more like solid membranes than 2D crystals.[5] The undulations are a consequence of the thermal fluctuations of the membrane. In this paper, we calculate these fluctuations quantitatively and discuss their implications upon the melting properties such as Lindemann parameter and melting temperature.[4] The results will be compared with corresponding 2D crystals.

The easiest way to estimate the melting temperature of a three-dimensional (3D) crystal is based on the Lindemann criterion.[6] According to it, a 3D crystal starts to melt when the square root of the thermal expectation value of lattice site elongations $\sigma_i \equiv \sqrt{\langle \mathbf{u}_i^2 \rangle_T}$ exceeds a certain fraction of the nearest-neighbor lattice distance a, usually around 0.1–0.15.[7] Above the melting temperature, the shear modulus of the lattice vanishes, leading to a divergence in the displacement fluctuations typical for the liquid state.

In 2Ds this criterion is no longer applicable since the displacement fluctuations are always logarithmically divergent, reflecting the fact that after a long time, a 2D crystal migrates through the entire 2D space. There exists, however, a simple modification.[8] Instead of $\langle \mathbf{u}_i^2 \rangle_T$ one may use the finite cumulants $\langle \mathbf{r}_{ij}^2 \rangle_T - \langle \mathbf{r}_{ij} \rangle_T^2$, where $\mathbf{r}_{ij}$ is the difference vector between the atoms associated with the nearest-neighbor lattice sites i and j. This leads to a modified Lindemann number,

$$\mathcal{L}_1^{s,2\mathrm{D}} = \frac{1}{|\mathcal{N}_1|} \sum_{i,j \in \mathcal{N}_1} \frac{\sqrt{\langle \mathbf{r}_{ij}^2 \rangle_T - \langle \mathbf{r}_{ij} \rangle_T^2}}{a}. \tag{1}$$

Here $\mathcal{N}_1$ denotes the set of all nearest-neighbor lattice pairs and $|\mathcal{N}_1|$ their number. For the Lennard-Jones and Wigner lattices, Bedanov *et al.*[8] found by computer simulations values of $\mathcal{L}_1^{s,2\mathrm{D}} \approx 0.15-0.2$. We have derived the same values analytically for a triangular generalization[9] of a square lattice defect melting model.[7]

At this point it is useful to realize that a migration problem and an associated divergence of σ_i exist also in three dimensions if the system is finite, i.e., for 3D clusters and polymers. There one defines a modified Lindemann number,

$$\mathcal{L}_{1,2}^{c} = \frac{1}{|\mathcal{N}_{1,2}|} \sum_{i,j \in \mathcal{N}_{1,2}} \frac{\sqrt{\langle \mathbf{r}_{ij}^2 \rangle_T - \langle r_{ij} \rangle_T^2}}{\langle r_{ij} \rangle_T}. \tag{2}$$

Here $\mathcal{N}_2$ is the set of *all* lattice site pairs whose number is $N(N-1)/2$ where N is the number of atoms in the lattice. The number $\mathcal{L}_1^c$ was introduced by Kaelberer and Etters,[10] the number $\mathcal{L}_2^c$ by Berry *et al.*[11] For small clusters, $\mathcal{L}_1^c$ and $\mathcal{L}_2^c$ have similar values[12] of around $\mathcal{L}_{1,2}^c \approx 0.03-0.05$ at the melting point. Above the melting point all modified Lindemann numbers increase considerably but do not go to infinity (this being in contrast to σ_i).

The main difference between $\mathcal{L}_1^{s,3\mathrm{D}}$ and $\mathcal{L}_1^c$ comes from the last term in the square root in Eqs. (1) and (2). Whereas $\langle \mathbf{r}_{ij} \rangle_T$ is the temperature average of the difference vector of sites i and j, i.e., $\mathbf{r}_{ij} = (x_{ij}, y_{ij}, z_{ij})$, the expectation value $\langle r_{ij} \rangle_T$ is the average value of the bonding length of sites i and j, i.e., $r_{ij} = (x_{ij}^2 + y_{ij}^2 + z_{ij}^2)^{1/2}$. Since $\mathbf{r}_{ij}^2 = r_{ij}^2$ one would expect that the 3D version of Eq. (1), $\mathcal{L}_1^{s,3\mathrm{D}}$, and $\mathcal{L}_1^c$ [Eq. (2)] could be equally useful in determining the melting point. This is indeed the case for 3D crystals.

In this paper we shall consider all three Lindemann numbers $\mathcal{L}_1^{s,3\mathrm{D}}$, $\mathcal{L}_1^c$, and $\mathcal{L}_2^c$ as candidates for a melting criterion for solid membranes such as graphene lattices or single-walled carbon nanotubes (SWNTs). It will turn out that for these $\mathcal{L}_1^{s,3\mathrm{D}}$ is unsuitable for calculating the melting temperature. The reason lies in the large out-of-plane fluctuations of the membrane varying little when crossing the melting point. These fluctuations cancel each other in Eq. (2) since $\langle z_{ij}^2 \rangle_T \neq 0$ and $r_{ij} \approx (x_{ij}^2 + y_{ij}^2)^{1/2} + (1/2) z_{ij}^2 / (x_{ij}^2 + y_{ij}^2)^{1/2}$ but not in $\mathcal{L}_1^{s,3\mathrm{D}}$ since $\langle z_{ij} \rangle_T = 0$.

Freely suspended graphene sheets are always undulated and behave like a solid membrane.[4] Nelson and Peliti[5] and Nelson *et al.*[13] showed that in-plane fluctuations tend to stabilize a solid membrane such that a flat phase can exist in spite of its large 2D fluctuations. The melting temperature of (5,5) SWNTs was determined by Zhang *et al.*[14] within numerical simulation to be around $T_m \approx 5000$ K, in agreement with experimental determinations.[15] The value of the Lindemann number $\mathcal{L}_2^c$ was around $\mathcal{L}_2^c \approx 0.03$ at the onset of melting defined by the abrupt increase in $\mathcal{L}_2^c$. However, when using the region of strong increase in the internal energy they obtain a range of $\mathcal{L}_2^c \approx 0.03 \sim 0.07$ from the onset of melting to its completion.

The shapes of SWNTs near the melting temperature are in general strongly deformed from a pure tube form. This leads to the conclusion that 2D nearest-neighbor Lindemann number $\mathcal{L}_1^{s,2D}$ (1) is not a useful quantity for a melting criterion. One rather should use Lindemann-type number (2) or the 3D form of Eq. (1) which both respect the 3D rotational symmetry of the system. In the following, we shall first calculate $\mathcal{L}_1^c$ which for small clusters and small supercells agrees in molecular dynamic simulations with $\mathcal{L}_2^c$. We shall restrict ourselves to the (5,5) SWNT so that we can compare our theoretical results with existing simulation data. We shall find that despite the large vertical fluctuations of the membranes, Lindemann number (2) depends mostly on the in-plane fluctuations and provides us with a valuable melting criterion. This is not the case for the 3D version of the Lindemann number $\mathcal{L}_1^s$ having its reason in the fact that the out-of plane fluctuations are even larger than the in-plane fluctuations for SWNTs and graphene. Surprisingly, the melting temperature of SWNTs is modified only a little by these large out-of-plane fluctuations at high temperatures.

II. MEMBRANES

The elastic energy of a solid elastic membrane in the flat phase is given by[16]

$$H_{\rm el} = \int d^2x \left[\mu u_{ij}^2 + \frac{1}{2}\lambda u_{ii}^2 + \sigma_{ij} u_{ij} + \frac{1}{2}\kappa_0 (\nabla_i \nabla_i f)^2 \right], \quad (3)$$

where

$$u_{ij} = \frac{1}{2}(\nabla_i u_j + \nabla_j u_i + \nabla_i f \nabla_j f) \quad (4)$$

and u_j are the lattice displacements in the xy plane, while f is the out-of-plane displacement. The constant μ is the shear modulus, and λ is the Lamé constant. The last term in Eq. (4) with the constant κ_0 accounts for the bending stiffness of the membrane. The quantity σ_{ij} is an external stress source which will help us to calculate Eqs. (1) and (2) from derivatives of the partition function with respect to σ_{ij}. The line element on the membrane for small distortions is given by[16] $dl'^2 = dl^2 + 2u_{ij} dx_i dx_j$, where dl is the length of the undistorted planar surface, which we identify with the equilibrium lengths l_{ij} between sites i and j. Thus we calculate $\mathcal{L}_{1,2}^c$ by first inserting the line element dl' in Eq. (2) and afterward by expanding the resulting expressions for small displacements. Thus we obtain

$$\mathcal{L}_{1,2}^c = \sum_{i,j \in \mathcal{N}_{1,2}} \frac{\sqrt{\langle (u_{lm} a^2 e_l^{ij} e_m^{ij})^2 \rangle_T - \langle u_{lm} a^2 e_l^{ij} e_m^{ij} \rangle_T^2}}{|\mathcal{N}_{1,2}| a^2}. \quad (5)$$

Here $\mathbf{e}^{ij}$ are the unit vectors pointing from site i to j. In deriving Eq. (5) we used a Taylor expansion of the elongation differences between two lattice sites (gradient expansion). This is justified for the small elongation differences of neighboring atoms occurring in $\mathcal{L}_1^s$ and $\mathcal{L}_1^c$ up to the melting regime. In the atom pairs summed over in $\mathcal{L}_2^c$, the approximation is good only for small clusters or for small supercells in molecular dynamic simulations. For infinite solid membranes, this is no longer the case. The contributions of the far separate pairs (i,j) cause a drastic decrease in the Lindemann parameter $\mathcal{L}_2^c$ with the size of the system. In a 2D crystal, for example, the widely separated pairs contribute terms which grow logarithmically with the separation: $\lim_{l_{ij}\to\infty} \langle \mathbf{r}_{ij}^2 \rangle_T - \langle \mathbf{r}_{ij} \rangle_T^2 \sim \ln l_{ij}$. This eliminates $\mathcal{L}_2^c$ for determining the melting point.

In order to calculate Eq. (5) we first integrate out the xy-lattice displacement fields u_i in the partition function, leading to an effective Hamiltonian $H = H_h + H_{\sigma\sigma}$ with

$$H_h = \int d^2x \left\{ \tilde{\mu}[(h_f + h_\sigma)^2 - h_\sigma^2] + \frac{1}{2}\kappa_0 (\nabla_i \nabla_i f) \right\},$$

$$H_{\sigma\sigma} = \int d^2x \left[\frac{1-\nu}{4\mu} \left(\frac{\nabla_i \nabla_j}{\nabla_l \nabla_l} \sigma_{ij} \right)^2 + \frac{1}{2\mu} \left(\frac{\nabla_i \nabla_j^T}{\nabla_l \nabla_l} \sigma_{ij} \right)^2 \right], \quad (6)$$

and the energy densities

$$h_f = \frac{1}{2} P_{lm}^T (\nabla_l f \nabla_m f),$$

$$h_\sigma = \frac{1}{2\mu} P_{lm}^T \left[1 - \delta_{lm} \frac{\nu}{1+\nu} \left(1 + \frac{\nabla_l \nabla_l}{(1-\delta_{lk}) \nabla_k \nabla_k} \right) \right] \sigma_{lm}. \quad (7)$$

In Eq. (6) we have used the abbreviation $\tilde{\mu} \equiv \mu(1+\nu) = E/2$ where E is the Young modulus and $\nu \equiv \lambda/(2\mu+\lambda)$ the Poisson ratio. The calculation of the energy densities in Eq. (7) is simplified by the fact that only the transverse part $P_{lm}^T \nabla_l f \nabla_m f$ with $P_{lm}^T = (\delta_{lm} - q_l q_m / q^2)$ of the out-of-plane fluctuations is relevant after integrating out the in-plane fields u_i.[5] The transverse projections lead to a useful restriction of the relevant phase space when calculating Feynman diagrams.

A. Self-consistent Born approximation

We now treat Hamiltonian (6) within the self-consistent Born approximation (SCBA) corresponding to the Hartree-Fock approximation for the eigenfunctions. Other approximations to Hamiltonian (6) have been used[17] to calculate the universal roughening exponents of the membrane, for example, in Ref. 18 an extension of SCBA.

Denoting the inverse Green's function of the f fluctuations by $G^{-1}(\mathbf{k}) = \kappa_0 k^4 + \Sigma(k)$, we obtain from Eq. (6) within the SCBA

$$\Sigma(k) = \frac{2\tilde{\mu}k_B T}{(2\pi)^2}\int_{\mathrm{BZ}} d^2q \frac{(\mathbf{k}\times\mathbf{q})^4}{q^4} G(\mathbf{k}+\mathbf{q}), \tag{8}$$

where we take into account only the Fock part of the SCBA. It was shown in Ref. 13 that the Hartree terms do not contribute for free boundary conditions of the xy elongations of the membrane. To do the integral in Eq. (8) we use a circular Brillouin zone (BZ) $k \leq k_{\mathrm{BZ}}$, with $k_{\mathrm{BZ}}=8\pi/\sqrt{3}a^2$ for the triangular Bravais lattice of SWNTs and graphene. Integral (8) can be carried out exactly for small k (Ref. 19) to obtain the first two terms in the expansion

$$\Sigma(k) = C_T k^3 + \kappa_\Sigma k^4 + \ldots, \tag{9}$$

where C_T is a temperature-dependent constant which turns out to be

$$\frac{C_T}{\kappa_0 k_{\mathrm{BZ}}} = \sqrt{\tilde{T}/2\pi}. \tag{10}$$

The symbol $\tilde{T}$ denotes the dimensionless temperature $\tilde{T} \equiv \tilde{\mu}k_B T/(\kappa_0 k_{\mathrm{BZ}})^2$.

The second coefficient κ_Σ is determined as follows. We assume that truncated small-k expansion (9) can be used for all k in the Brillouin zone, implying that the inverse Green's function has the form

$$G^{-1}(\mathbf{k}) \approx C_T k^3 + \kappa_r k^4, \tag{11}$$

with $\kappa_r \equiv \kappa_0 + \kappa_\Sigma$. We shall see below that this assumption is indeed justified. At low temperature where $C_T \ll \kappa_r k_{\mathrm{BZ}}$ we determine κ_r by inserting Eq. (11) into Eq. (8) and evaluating the integral for $\Sigma(k)$ at the momentum $k=C_T/\kappa_r$. This momentum regime is most relevant in the integrals over G which we have to calculate in the following in order to determine the generalized Lindemann parameters. Moreover, we will show below that Eq. (8) is then justified in good approximation for momenta even in the whole Brillouin zone. At higher temperatures where $C_T \gg \kappa_r k_{\mathrm{BZ}}$, we determine κ_r by integrating Eq. (8) at $k=k_{\mathrm{BZ}}$. In both temperature regimes we carry the momentum integrations up to $k=k_{\mathrm{BZ}}$ and obtain in either case a quadratic equation for κ_r, solved by

$$\frac{\kappa_r}{\kappa_0} \approx \begin{cases} \dfrac{3\tilde{T}}{8\pi}\left(1-\sqrt{1-\dfrac{15}{16\pi}\tilde{T}}\right)^{-1}, & \text{for } C_T \ll \kappa_r k_{\mathrm{BZ}}, \\ 1-\dfrac{3}{4\sqrt{2\pi}}\sqrt{\tilde{T}}, & \text{for } C_T \gg \kappa_r k_{\mathrm{BZ}}. \end{cases} \tag{12}$$

Our approximations are justified in Fig. 1 showing in the main plot the quantity $G^{-1}(k) \equiv \kappa_r k^4 + C_T k^3$ divided by the sum of $\kappa_0 k^4$ and the numerically integrated right-hand side of self-energy function (8). The numbers on the curves are the various dimensionless temperatures $\tilde{T}$. Observing that the values of these curves are almost constant and equal to unity confirms that $G(k)$ of Eq. (11) indeed fulfills almost exactly the SCBA [Eq. (8)]. The inset of Fig. 1 shows κ_r/κ_0 as a function of the dimensionless temperature $\tilde{T}$ calculated either by Eq. (12), corresponding in the figure to the (green) solid and dashed curves, or by the determination of κ_r/κ_0 by numerical integration of the right-hand side of Eq. (8) [(blue) dashed-dotted curve]. The kink in this curve corresponds to parameter values where $C_T/\kappa_r k_{\mathrm{BZ}}=1$. Note that for graphene and SWNTs we have $\tilde{T}_m \approx 1.34$ at the melting point $T_m \approx 5000$ K.

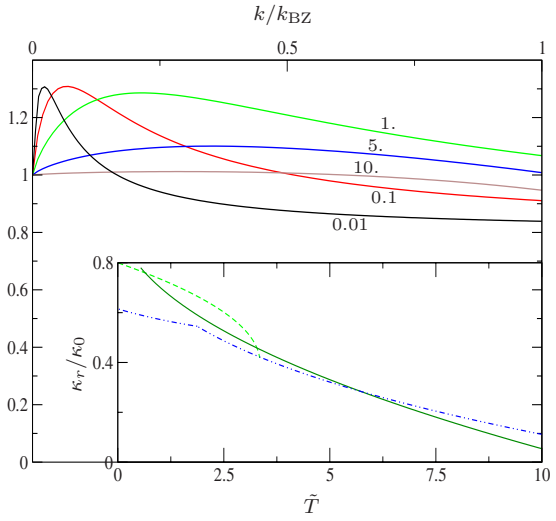

FIG. 1. (Color online) Upper figure shows $G^{-1}(k) \approx C_T k^3 + \kappa_r k^4$ divided by the sum of $\kappa_0 k^4$ and the numerical integrated right-hand side of self-energy function (8) where we used $G^{-1}(k)=C_T k^3 + \kappa_r k^4$. The numbers at the curves are the dimensionless temperatures $\tilde{T}$. The inset shows the $\tilde{T}$ behavior of κ_r/κ_0. The low-temperature dashed curve represents Eq. (12) in the regime $C_T \ll \kappa_r k_{\mathrm{BZ}}$, the high-temperature solid curve in the regime $C_T \gg \kappa_r k_{\mathrm{BZ}}$. The dashed-dotted curve pictures the ratio κ_r/κ_0 obtained from Eq. (8) by numerical integration of the right-hand side with $G^{-1}(k)=C_T k^3 + \kappa_r k^4$.

Next we calculate the expectation value $\langle \nabla_i f \nabla_j f \rangle$ where the average is taken with respect to the Gibbs measure of Hamiltonian (3) or (6), respectively. In SCBA, this leads to

$$\langle \nabla_i f \nabla_j f \rangle_T \approx \frac{1}{(2\pi)^2}\int_{\mathrm{BZ}} d^2k k_i k_j G(k) = \delta_{ij}\frac{\tilde{T}}{4\pi}\frac{\kappa_0 k_{\mathrm{BZ}}^2}{\tilde{\mu}}\frac{\kappa_0}{\kappa_r}\ln\left(1+\frac{\kappa_r k_{\mathrm{BZ}}}{C_T}\right). \tag{13}$$

Recalling Eq. (4) we observe that the strain in the xy plane is on the average equal to the negative of Eq. (13): $\langle \nabla_j u_i + \nabla_i u_j \rangle_T = -\langle \nabla_i f \nabla_j f \rangle_T$, implying that the self-induced stress due to thermal out-of-plane fluctuations vanishes.

B. Lindemann numbers

We are now prepared to calculate $(\mathcal{L}_1^c)^2$ of Eq. (5) by differentiating the partition function of the elastic Hamiltonian H_{el} twice with respect to the stress source σ_{ij} and setting $\sigma_{ij}=0$ at the end. Going over to effective Hamiltonian (6) we obtain two contributions $(\mathcal{L}_1^c)^2=(\mathcal{L}_1^{s,2\mathrm{D}})^2+\mathcal{L}_{z1}^2$, where the first is the square of Lindemann number (1) for the 2D hexagonal solid given by

$$(\mathcal{L}_1^{s,2D})^2 = \frac{1}{2}(\langle \nabla_i u_m \nabla_i u_m \rangle_{2D} - \langle \nabla_i u_m \rangle_{2D} \langle \nabla_i u_m \rangle_{2D}) \approx \frac{k_B T}{\mu} \frac{3-\nu}{8} k_{BZ}^2. \tag{14}$$

The average $\langle \cdots \rangle_{2D}$ is calculated with respect to the Gibbs measure of Hamiltonian (3) with $f=0$ corresponding to the 2D crystal. This contribution to $(\mathcal{L}_1^c)^2$ comes from the derivate of $H_{\sigma\sigma}$ in Eq. (6) with respect to σ_{ij}. The second contribution $\mathcal{L}_{z1}^2$ has its origin in the derivates of the h_h term in Eq. (6) with respect to σ_{ij} and is found to be

$$\mathcal{L}_{z1}^2 = (1+\nu)^2 \frac{1}{2(2\pi)^2} \int_{BZ} d^2q \frac{1}{q^4} \left(q_i q_j - \delta_{ij} \frac{\nu}{1+\nu} q^2 \right)^2 I(q), \tag{15}$$

where $I(q)$ is the Fourier transform of the h_f^4 correlator $\langle h_f(x) h_f(x') \rangle_T - \langle h_f(x) \rangle_T \langle h_f(x') \rangle_T$. Within self-consistent Born approximation we have

$$I(q) = \frac{(k_B T)^2}{2(2\pi)^2} \int_{BZ} d^2k \frac{(\mathbf{k} \times \mathbf{q})^4}{q^4} G(\mathbf{k}+\mathbf{q}) G(\mathbf{k}) \Lambda(\mathbf{k}+\mathbf{q}, \mathbf{k}). \tag{16}$$

The vertex correction factor $\Lambda(\mathbf{k}+\mathbf{q}, \mathbf{k})$ is required within the SCBA by charge-current conservation. We first calculate Eq. (16) in the lowest approximation $\Lambda \approx 1$, to be justified below. By using analytic approximation (11) we obtain for Eq. (15) with Eq. (16) by integration[19]

$$\mathcal{L}_{z1}^2 \approx \begin{cases} \frac{3(1+\tilde{\nu})^2}{32(2\pi)^2} \tilde{T}^2 \left(\frac{\kappa_0^2 k_{BZ}^2}{\kappa_r \tilde{\mu}} \right)^2 \ln \frac{\kappa_r k_{BZ}}{C_T}, & C_T \ll \kappa_r k_{BZ}, \\ 0.3 \frac{3(1+\tilde{\nu})^2}{32(2\pi)^2} \tilde{T}^2 \left(\frac{\kappa_0 k_{BZ}^2}{\tilde{\mu}} \right)^2 \left(\frac{\kappa_0 k_{BZ}}{C_T} \right)^2, & C_T \gg \kappa_r k_{BZ}, \end{cases} \tag{17}$$

with $(1+\tilde{\nu})^2 = (1+\nu)^2 \{1 - 2[\nu/(1+\nu) - \nu^2/(1+\nu)^2]\}$.

Our results depend strongly on the number of the 2D Young modulus $E \equiv 2\tilde{\mu}$. The literature gives a broad range of possible $\tilde{\mu}$ values (see, for example, Refs. 20 and 21, and references therein) which makes the comparison of our results with experiment nonstraightforward. It was shown by Hsieh *et al.*[20] using a molecular dynamics simulation that the Young modulus of (5,5) SWNTs is softened near the melting temperature to around 70% of the $T=0$ value, in agreement with Dereli and Süngü[21] where a simulation of the larger (10,10) SWNT was carried out. This value for the temperature reduction is in accordance with the temperature reduction of the 2D Young modulus in Wigner crystals[22] at melting determined by computer simulation. This can be generalized by theoretical arguments to softening expressions of elastic moduli[7,9] for 2D crystals in general. The $T=0$ value for the (5,5) SWNT determined by Hsieh *et al.*[20] is $E \approx 660$ N/m and lies at the upper end of existing Young moduli in the literature. On the other hand the simulation of Dereli *et al.*[20] for the (10,10) SWNT results in a much lower value at room temperature of around $E \approx 140$ N/m where it should not much differ to its $T=0$ value[20] lying at the lower end of existing Young moduli for SWNTs in the literature. One should compare this value with the value $E \approx 440$ N/m found by Hsieh *et al.*[20] for the (17,0) tube, taking into account that the Young modulus depends only on the diameter of the tube and not on the helicity[20] in first approximation. The origin of these discrepancies in the Young modulus values shown in the literature in general is not clear yet.

To compare our analytic results with the simulation results of Zhang *et al.*[14] we shall use in the following the $T=0$ value $E \approx 350$ N/m for the (5,5) SWNT which is in the immediate proximity of several simulations (see Ref. 23, and references therein) and experimental values.[24] The associated softened 2D Young modulus for (5,5) SWNTs is thus $E \approx 245$ N/m, which will be used in the rest of the paper. The remaining parameters are less significant for our results. We shall take $\nu \approx 0.14$, $\kappa_0 \approx 0.16 \times 10^{-18}$ N m, and $k_{BZ}^2 \approx 2.46 \times 10^{20}/\mathrm{m}^2$ which are typical for SWNTs and graphene. Inserting these material parameters we obtain for the melting temperature[14] $T_m = 5000$ K a value of $\mathcal{L}_z^2 \approx 5.6 \times 10^{-4}$. Contribution (14), on the other hand, adds to this $(\mathcal{L}_1^{s,2D})^2 \approx 8.9 \times 10^{-3}$ at $T_m \approx 5000$ K so that the modified Lindemann number $\mathcal{L}_1^c$ is $\approx \mathcal{L}_1^{s,2D} \approx 0.09$. This lies in the range of values $\mathcal{L}_2^c \approx 0.03-0.07$ obtained by numerical simulation.[14]

Our calculation shows that the abrupt increase in $\mathcal{L}_1^c$ is a meaningful criterion for the determination of the melting point. At the melting point, the in-plane shear modulus μ will drop to zero, where according to Eqs. (14) and (17), $\mathcal{L}_1^{s,2D}$ goes to infinity.

Next we calculate the 3D form of Eq. (1) $(\mathcal{L}_1^{s,3D})^2 = (\mathcal{L}_1^{s,2D})^2 + \mathcal{L}_{z1}^2 + \mathcal{L}_{z2}^2 + \frac{1}{2}\langle \nabla_i f \nabla_i f \rangle_T$, where the last term is due to nearest-neighbor out-of-plane fluctuations given by Eq. (13). The first three terms measure in-plane fluctuations where $\mathcal{L}_{z2}^2$ is given by the momentum integral

$$\mathcal{L}_{z2}^2 = -2(1+\nu) \frac{1}{2(2\pi)^2} \int_{BZ} d^2q \frac{1}{q^2} \left[(2\delta_{ij} - 1) q_i q_j - \delta_{ij} \frac{\nu}{1+\nu} q^2 \right] I_{ij}^1(q) + \frac{1}{2(2\pi)^2} \int_{BZ} d^2q I_{ij,ij}^2(q). \tag{18}$$

The functions $I_{ij}^1(q)$ and $I_{ij,ij}^2(q)$ denote the Fourier transforms of the expectation values

$$\frac{1}{2}[\langle \nabla_i f(x) \nabla_j f(x) h_f(x') \rangle_T - \langle \nabla_i f(x) \nabla_j f(x) \rangle_T \langle h_f(x') \rangle_T]$$

and

$$\frac{1}{4}[\langle \nabla_i f(x) \nabla_j f(x) \nabla_i' f(x') \nabla_j' f(x') \rangle_T - \langle \nabla_i f(x) \nabla_j f(x) \rangle_T \langle \nabla_i' f(x') \nabla_j' f(x') \rangle_T],$$

respectively. The contribution $\mathcal{L}_{z2}^2$ is calculated in the same way as $\mathcal{L}_{z1}^2$,[19] yielding

$$\mathcal{L}_{z2}^2 \approx \begin{cases} \frac{3}{16(2\pi)^2}\tilde{T}^2\left(\frac{\kappa_0^2 k_{\mathrm{BZ}}^2}{\kappa_r\tilde{\mu}}\right)^2 \ln^2\left(\frac{\kappa_r k_{\mathrm{BZ}}}{C_T}\right), & C_T \ll \kappa_r k_{\mathrm{BZ}}, \\ \frac{3(1+\tilde{\tilde{\nu}})}{16(2\pi)^2}\tilde{T}^2\left(\frac{\kappa_0 k_{\mathrm{BZ}}^2}{\tilde{\mu}}\right)^2\left(\frac{\kappa_0 k_{\mathrm{BZ}}}{C_T}\right)^2, & C_T \gg \kappa_r k_{\mathrm{BZ}}. \end{cases} \tag{19}$$

Here we have used the abbreviation $(1+\tilde{\tilde{\nu}}) \equiv 1 + (1+\nu)[-0.31+0.25\nu/(1+\nu)]$. Using the material parameters of SWNTs and graphene given above, we find that the main contribution to $\mathcal{L}_1^{s,3\mathrm{D}}$ comes from the out-of-plane fluctuations and is given by $\mathcal{L}_1^{s,3\mathrm{D}} \approx (\langle \nabla_i f \nabla_i f \rangle_T/2)^{1/2} \approx 0.22$ at the melting point $T_m \approx 5000$ K. Thus, we find that the out-of-plane fluctuations $(\langle \nabla_i f \nabla_i f \rangle_T/2)^{1/2}$ are even larger than the dominant contribution to the in-plane fluctuations $\mathcal{L}_1^{s,2\mathrm{D}}$. By comparing temperature dependence (13) with Eq. (14) we obtain that this is even the case for smaller temperatures. Furthermore, we realize that in contrast to the Lindemann number $\mathcal{L}_1^c$, the abrupt increase in the Lindemann number $\mathcal{L}_1^{s,3\mathrm{D}}$ gives no good signal for the melting point of a solid membrane. The reason is that the vanishing elastic shear modulus μ at melting contributes in two ways to the dominant fluctuation term $\langle \nabla_i f \nabla_i f \rangle_T/2$ [Eq. (13)], but neither of them changes this value much at melting. First, the out-of-plane fluctuations depend on μ via κ_r/κ_0 and remains finite for $\mu \to 0$, and second they depend pickup logarithmic dependence on μ from $C_T/\kappa_0 k_{\mathrm{BZ}}$.

Consider now the higher-order vertex corrections collected in the factor $\Lambda(\mathbf{k}+\mathbf{q},\mathbf{k})$ in Eq. (16). First we note that for $\Lambda \equiv 1$ we obtain $2\tilde{\mu} I(q)/k_B T < 3/8$ in the dominant integration regime of Eq. (15) near $q \approx C_T/\kappa$ for $C_T \ll \kappa_r k_{\mathrm{BZ}}$ and near $q \approx k_{\mathrm{BZ}}$ for $C_T \gg \kappa_r k_{\mathrm{BZ}}$. The factor 3/8 comes mainly from the reduction in the phase space integral by the projections P^T in the polarisator. We expect that the nth order in Λ contributes roughly with a factor $[2\tilde{\mu} I(q)/k_B T]^n$ to $I(q)$ in the dominant integration regime of Eq. (15) due to the additional phase space projection terms P^T. We have checked this explicitly by taking into account first-order corrections in the vertex Λ in Eq. (16). A similar suppression of higher-order vertex correction contributions occurs in $I_{ij}^1(q)$ and $I_{ijij}^2(q)$.

C. Melting temperature

Let us finally discuss the impact of the large out-of-plane fluctuations upon the melting temperature. In Ref. 9, we have calculated the melting temperature of a 2D triangular lattice approximately from the intersection of high- and low-temperature expansions of the free energies associated with Hamiltonian (3) with zero vertical displacements $f(\mathbf{x})$. The transition was caused by integer-valued defect gauge fields accounting for the plastic deformations of the crystal in the xy plane. These are coupled minimally to the xy-displacement fields $u_i(\mathbf{x})$. In that theory, the melting temperature T_m was found to obey the equation

$$\tilde{\beta} \equiv \frac{1}{k_B T_m}\frac{\tilde{\mu}}{(2\pi)^2} v_F \approx 0.6, \tag{20}$$

where $v_F \equiv \sqrt{3}a^2/2$ denotes the 2D volume (area) of the fundamental cell. In SWNTs and graphene, this result is modified by a factor Se^{-2W}, where S is a structure factor and e^{-2W} a Debye-Waller-type factor caused by the out-of-plane fluctuations $f(\mathbf{x}) \neq 0$. The honeycomb lattice of SWNTs contains two atoms per triangular fundamental cell leading to a structure factor $S=1/2$. To estimate the size of e^{-2W} we observe that in the defect melting model, the defect gauge field appears at a similar place as the vertical distortion $\nabla_i f \nabla_j f/2$ in Hamiltonian (3). Thus one can immediately write down the Hamiltonian H_h of Eq. (6) coming from defects. This leads to the low-temperature expansion of the partition function. In the high-temperature expansion, there exists a dual stress representation of the partition function.[7,9] In both low- and high-temperature representations, the coupling terms between the defect fields or the stress fields to the out-of-plane fluctuations $f(\mathbf{x})$ are smaller than the pure defect and stress term by approximately a factor of $(4\pi^2\tilde{\beta})^2\mathcal{L}_{z1}^2$ and $(2\pi)^2\mathcal{L}_{z2}^2$, respectively. When neglecting these small coupling terms we find that the partition function receives a sizable correction factor only in the low-temperature approximation due to the Fock energy of the Hamiltonian H_h. The Hartree energy is missing as a consequence of the open-boundary conditions on the membrane.[13] From these considerations we obtain

$$\begin{aligned} W &= \frac{v_F}{4}\frac{1}{(2\pi)^2}\int_{\mathrm{BZ}} d^2k \Sigma(k) G(k) \\ &= \frac{1}{2}\frac{C_T}{\kappa_r k_{\mathrm{BZ}}}\left[1 - \frac{C_T}{\kappa_r k_{\mathrm{BZ}}}\ln\left(1+\frac{\kappa_r k_{\mathrm{BZ}}}{C_T}\right)\right] \\ &\quad + \frac{1}{2}\left(1-\frac{\kappa_0}{\kappa_r}\right)\left[\frac{1}{2} - \frac{C_T}{\kappa_r k_{\mathrm{BZ}}} + \left(\frac{C_T}{\kappa_r k_{\mathrm{BZ}}}\right)^2 \ln\left(1+\frac{\kappa_r k_{\mathrm{BZ}}}{C_T}\right)\right]. \end{aligned} \tag{21}$$

Using the parameters above for (5,5) SWNTs we obtain $W \approx 0.06$ at $T \approx 5000$ K. The factor e^{-2W} gives thus only a small correction to the melting temperature determined by Eq. (20). The explicit evaluation of that equation yields a melting temperature $T_m \approx 8000$ K $(W \approx 0.075)$, somewhat larger than the melting temperature $T_m \approx 5000$ K of Zhang *et al.*[14] obtained by numerical simulation.

III. CONCLUSION

In this paper we have calculated the fluctuations of solid membranes such as graphene and single-walled carbon nanotubes with the help of the self-consistent Born approximation. Our results show that the out-of plane fluctuations are much larger than the in-plane fluctuations even at low temperatures. Thus they may be expected to have dramatic consequences for the Lindemann numbers as well as the melting temperature of solid membranes in comparison to 2D crystals. Surprisingly, for the melting temperature this expectation was not confirmed. The fluctuations was discussed by evaluating the 3D version $\mathcal{L}_1^{s,3\mathrm{D}}$ of Lindemann number (1),

originally introduced to estimate the melting temperature of 2D solids, and the Lindemann number $\mathcal{L}_1^c$ defined in Eq. (2), originally introduced in cluster physics. We observed that a Lindemann criterion based on $\mathcal{L}_1^c$ is more reliable than that-based on the former. The associated Lindemann number is dominated by in-plane fluctuations, in contrast to the former which is dominated by the large out-of-plane fluctuations. By calculating, in addition, the melting temperature from a simple defect model of melting for single-walled carbon nanotubes and graphene [Eq. (20)] we observed in contrast to the expectation that the melting temperature depends only very little on the large out-of-plane fluctuations.

ACKNOWLEDGMENT

The authors acknowledge the support by Deutsche Forschungsgemeinschaft under Grant No. KL 256/42-2.

[1] K. S. Novoselov, A. K. Geim, A. K. Geim, S. V. Morozov, D. Jiang, Y. Zhang, S. V. Dubonos, I. V. Grogorieva, and A. A. Firsov, Science **306**, 666 (2004).
[2] K. S. Novoselov, D. Jiang, F. Schedin, T. J. Booth, V. V. Khotkevich, S. V. Morozov, and A. K. Geim, Proc. Natl. Acad. Sci. U.S.A. **102**, 10451 (2005).
[3] S. Iijima, Nature (London) **354**, 56 (1991).
[4] J. C. Meyer, A. K. Geim, M. I. Katsnelson, K. S. Novoselov, T. J. Booth, and S. Roth, Nature (London) **446**, 60 (2007).
[5] D. R. Nelson and L. Peliti, J. Phys. (Paris) **48**, 1085 (1987).
[6] F. A. Lindemann, Phys. Z. **11**, 609 (1910).
[7] H. Kleinert, *Gauge Fields in Condensed Matter—Stresses and Defects: Differential Geometry, Crystal Melting* (World Scientific, Singapore, 1989), Vol. 2 (readable online at www.physik.fu-berlin.de/~kleinert/re.html#b2).
[8] V. M. Bedanov, G. V. Gadiyak, and Y. E. Lozovik, Phys. Lett. **109A**, 289 (1985).
[9] J. Dietel and H. Kleinert, Phys. Rev. B **73**, 024113 (2006).
[10] J. B. Kaelberer and R. D. Etters, J. Chem. Phys. **66**, 3233 (1977).
[11] R. S. Berry, T. L. Beck, H. L. Davis, and J. Jellinek, Adv. Chem. Phys. **70**, 75 (1988).
[12] Y. Zhou, M. Karplus, K. D. Ball, and R. S. Berry, J. Chem. Phys. **116**, 2323 (2002).
[13] *Statistical Mechanics of Membranes and Surfaces*, edited by D. R. Nelson, T. Piran, and S. Weinberg (World Scientific, Singapore, 2004).
[14] K. Zhang, G. M. Stocks, and J. Zhong, Nanotechnology **18**, 285703 (2007).
[15] J. Y. Huang, S. Chen, Z. F. Ren, Z. Q. Wang, D. Z. Wang, M. Vaziri, Z. Suo, G. Chen, and M. S. Dresselhaus, Phys. Rev. Lett. **97**, 075501 (2006).
[16] L. D. Landau and E. M. Lifshitz, *Electrodynamics of Continuous Media (Course of Theoretical Physics)* (Pergamon, Oxford, 1960), Vol. 8.
[17] M. J. Bowick and A. Travesset, Phys. Rep. **344**, 255 (2001).
[18] P. LeDoussal and L. Radzihovsky, Phys. Rev. Lett. **69**, 1209 (1992).
[19] V. A. Smirnov, *Evaluating Feynman Integrals* (Springer, Berlin, 2004).
[20] J.-Y. Hsieh, J.-M. Lu, M.-Y. Huang, and C.-C. Hwang, Nanotechnology **17**, 3920 (2006).
[21] G. Dereli and B. Süngü, Phys. Rev. B **75**, 184104 (2007).
[22] R. H. Morf, Phys. Rev. Lett. **43**, 931 (1979).
[23] Y. Huang, J. Wu, and K. C. Hwang, Phys. Rev. B **74**, 245413 (2006).
[24] J. P. Lu, Phys. Rev. Lett. **79**, 1297 (1997).